Improving robustness to termination conditions in passivity enforcement of rational macromodels

Improving robustness to termination conditions in passivity enforcement of rational macromodels

Antonio Carlucci, *Graduate Student Member, IEEE*, Tommaso Bradde, *Member, IEEE*, Stefano Grivet-Talocia, *Fellow, IEEE*

***Abstract*—Common design and verification flows of electronic systems under Signal and/or Power Integrity (SI/PI) constraints often rely on the availability of accurate macromodels of components and interconnects. Such macromodels enable fast transient analysis at the system level and consequently the possibility to efficiently verify the quality of the design. Several approaches are available to construct macromodels whose response accurately matches the raw data used for their identification, most often tabulated scattering responses. However, for the sake of SI/PI optimization, it is mandatory that such models reproduce accurately the underlying structure response when inserted as a component in a larger network, possibly subjected to different or uncertain port termination schemes. This capability is not inherently guaranteed by standard macromodeling approaches. Recently, the authors proposed a modified Vector Fitting (VF) iteration that overcomes this issue, by optimizing the macromodel accuracy with respect to sets of arbitrary terminations. This work completes this robust macromodeling framework by introducing a companion perturbation-based passivity enforcement scheme that preserves the macromodel accuracy with respect to the prescribed set of loads. The main innovation is the definition of a novel loss function to drive the perturbation routine, that allows to correct the non-passive model while preserving the required robust performance. Numerical evidence on a set of relevant Power Delivery Network (PDN) benchmarks confirms the effectiveness of the proposed approach.**

I. Introduction

Transient analysis of large-scale circuits is a mandatory step for verifying and optimizing the electrical performance of modern electronic systems, in particular for Signal Integrity (SI) and Power Integrity (PI) applications. Although for a given design many performance indices can be inferred based on frequency domain descriptions, time domain analysis represents the ultimate verification tool, especially when active/nonlinear devices are involved [1]–[3].

Very efficient transient analyses are typically enabled by representing the behavior of complex interconnects and components via state-space macromodels, whose extraction from tabulated scattering data from electromagnetic solvers is nowadays considered an off-the-shelf commodity [4]. Among all methods, the rational approximation method known as Vector Fitting (VF) iteration currently represents the reference algorithm. Since the first appearance of VF [5], significant improvements have been proposed in the literature in order to increase its robustness [6]–[9], efficiency [10]–[13], and accuracy [14], as well as for extending the original frequency domain formulation to time domain measurements [15], [16] or to a more general multivariate setting [17]. Correspondingly, a number of available methods have been proposed to enforce the passivity of the resulting macromodels [18]–[23]. This Passivity Enforcement (PE) step is fundamental, since a non-passive macromodel may induce spurious numerical instabilities when included in transient simulations in which it is interconnected with other (even passive) electrical networks [24]. For a comprehensive overview on passive macromodeling and its applications see [4].

Macromodels are never solved as standalone components. Instead, they are typically inserted in a global network description as individual components, whose ports are interconnected to other components and subsystems to obtain a complete computational model of an entire system. Examples can be Power Delivery Network (PDN) models at board, package and chip level which are interconnected and loaded by decoupling capacitor banks, possibly integrated voltage regulator models with sense and feedback loops, and excited by chip loading patterns [25], [26]. The main objective of system-level transient verification is an accurate prediction of all port signals of such coupled and terminated global system. The accuracy of a single macromodel is not important by itself, but rather as an enabler for an accurate prediction of the entire system behavior.

One relevant open problem affecting the above described framework is related to the *sensitivity* of the passive macromodels to their actual operating conditions. As pointed out in a number of papers [27]–[32], even when a macromodel matches with high accuracy one network function of the underlying component, it is not formally guaranteed that it will reproduce the desired port behavior when loaded with an arbitrary electrical network. Intuitively, this happens because the (even small) residual error affecting the macromodel response propagates through the feedback loops that arise from the electrical interconnections and terminations, undergoing uncontrolled and possibly large magnification. Although often overlooked, the macromodel sensitivity in not uncommon in scenarios of practical interests, and especially in PI applications [30]–[32].

In the recent papers [31], [32], the authors proposed to alleviate the problem by optimizing the macromodel accuracy with respect to a prescribed (yet completely arbitrary) class of Linear and Time-Invariant (LTI) terminations. The approach modifies the VF iteration, by explicitly incorporating in the optimization routine the information about the port behavior of the system under modeling when it is subjected to the

A. Carlucci, T. Bradde, and S. Grivet-Talocia are with the Dept. of Electronics and Telecommunications, Politecnico di Torino, C. Duca degli Abruzzi 24, 10129 Torino, Italy (email: antonio.carlucci@polito.it, tommaso.bradde@polito.it, stefano.grivet@polito.it).

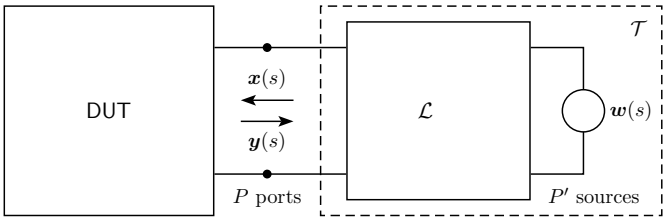

Fig. 1. General system topology under investigation, where the DUT is connected to a loading network $\mathcal{L}$ with external excitations $\boldsymbol{w}$. Variables $\boldsymbol{x}$ and $\boldsymbol{y}$ denote input and output signals of the DUT, respectively.

admissible loads. It was verified that this strategy generates macromodels that are more robust, in the sense that their accuracy is less sensitive when the port terminations are changed. In this work, we build on these results, and we augment the proposed framework with an ad hoc passivity enforcement post-processing algorithm that preserves robustness to port loading conditions. The proposed approach inherits the strategy applied in most of the perturbation-based passivity enforcement algorithms [18]–[22], [33]. Starting from a non-passive rational model, we perturb its residues iteratively in order to achieve passivity, by solving a constrained optimization problem that minimizes model perturbation subject to passivity constraints. Robustness to loading conditions is here enforced by suitable penalization terms added to the cost function defining model accuracy. Several examples, mostly related to PI applications, are presented to demonstrate the excellent performance of this approach, despite its simplicity in both formulation and implementation.

This manuscript is structured as follows. Section II introduces preliminaries and notation. Background on robust macromodeling is presented in Sec. III. The proposed robust passivity enforcement scheme is discussed in Sec. IV, and numerical examples are presented in Sec. V.

II. Notation and preliminaries

In the following, scalars will be denoted with lowercase italic fonts (x); vectors and matrices with bold italic fonts, lowercase ($\boldsymbol{x}$) and uppercase ($\mathbf{X}$) respectively. The notation $\mathbf{X}^\mathsf{T}$ and $\mathbf{X}^*$ represents the matrix transpose and the hermitian transpose of $\mathbf{X}$. The symbol $\mathbb{I}_P$ is the identity matrix of size P. With $\mathbf{A} \otimes \mathbf{B}$ we denote the Kronecker product between matrices $\mathbf{A}$ and $\mathbf{B}$ and operator $\mathrm{vec}\{\cdot\}$ stacks the elements of its matrix argument as a column vector. The imaginary unit is $j = \sqrt{-1}$ and the Laplace variable is $s = \sigma + j\omega$. The matrix norm notation $\|\mathbf{X}\|$ indicates the 2-norm, whereas $\|\mathbf{X}\|_F$ is the Frobenius norm. Similarly, for vectors, $\|\boldsymbol{x}\|$ is the standard Euclidean norm. We recall that $\|\mathbf{X}\|_F = \|\mathrm{vec}\{\mathbf{X}\}\|$.

Let us consider an arbitrary passive LTI P-port network, labeled as Device Under Test (DUT) in Fig. 1. An external port representation for the DUT can be given in terms of one of its network functions, e.g. its impedance, admittance, or scattering matrices. We will generically denote a network function of the DUT as $\breve{\mathbf{H}}(s) \in \mathbb{C}^{P\times P}$. Correspondingly, we will denote with $\breve{\boldsymbol{x}}(s) \in \mathbb{C}^P$ and with $\breve{\boldsymbol{y}}(s) \in \mathbb{C}^P$ the input and the output signals associated with this network representation, so that

$$\breve{\boldsymbol{y}}(s) = \breve{\mathbf{H}}(s)\breve{\boldsymbol{x}}(s). \tag{1}$$

The accent $\breve{}$ is used to label the *exact* network function of the DUT and its port signals, whereas any DUT quantity without accents will correspond to the (approximate) models to be constructed with related port signals.

With reference to Fig. 1, we will consider the scenario in which the DUT is a subnetwork of a larger interconnected system. Without loss of generality, we assume the DUT is connected with an arbitrary loading LTI network $\mathcal{L}$, having P ports connected to the DUT and P' ports excited by ideal voltage or current sources. We will collect these sources in the vector $\boldsymbol{w}(s)$. Considering a representation of $\mathcal{L}$ based on the same DUT port signals, we can write

$$\breve{\boldsymbol{x}}(s) = \boldsymbol{\Gamma}(s)\breve{\boldsymbol{y}}(s) + \mathbf{P}(s)\boldsymbol{w}(s) \tag{2}$$

where matrices $\boldsymbol{\Gamma}(s)$ and $\mathbf{P}(s)$ are supposed to be known. Combining (1) with (2) leads to the exact solution of the coupled system for the interface port signals

$$\breve{\boldsymbol{x}}(s) = [\mathbb{I}_P - \boldsymbol{\Gamma}(s)\breve{\mathbf{H}}(s)]^{-1}\mathbf{P}(s)\boldsymbol{w}(s) \tag{3a}$$

$$\breve{\boldsymbol{y}}(s) = \breve{\mathbf{H}}(s)[\mathbb{I}_P - \boldsymbol{\Gamma}(s)\breve{\mathbf{H}}(s)]^{-1}\mathbf{P}(s)\boldsymbol{w}(s). \tag{3b}$$

III. Robust Macromodeling

The objective of this paper is to describe a procedure for the generation of a passive macromodel $\mathbf{H}(s)$ that reproduces the DUT behavior not only by matching its exact network function

$$\mathbf{H}(s) \approx \breve{\mathbf{H}}(s) \tag{4}$$

as typical in standard macromodeling schemes, but also when the model replaces the DUT in its operating environment, as in Fig. 1. This requirement is not trivial: while enforcing (4) is straightforward with state-of-the-art passive macromodeling approaches [4], ensuring that the port signals

$$\boldsymbol{x}(s) = [\mathbb{I}_P - \boldsymbol{\Gamma}(s)\mathbf{H}(s)]^{-1}\mathbf{P}(s)\boldsymbol{w}(s) \tag{5a}$$

$$\boldsymbol{y}(s) = \mathbf{H}(s)[\mathbb{I}_P - \boldsymbol{\Gamma}(s)\mathbf{H}(s)]^{-1}\mathbf{P}(s)\boldsymbol{w}(s), \tag{5b}$$

obtained by replacing the exact DUT with its macromodel, match up to the desired accuracy their references (3)

$$\boldsymbol{y}(s) \approx \breve{\boldsymbol{y}}(s), \quad \boldsymbol{x}(s) \approx \breve{\boldsymbol{x}}(s) \tag{6}$$

requires additional care. This difficulty is evident from (3), basically due to the matrix $[\mathbb{I}_P - \boldsymbol{\Gamma}(s)\breve{\mathbf{H}}(s)]$ that needs to be inverted. When such matrix is nearly singular with some small magnitude eigenvalue μ, the inevitable approximation error $\Delta\mathbf{H}(s) = \mathbf{H}(s) - \breve{\mathbf{H}}(s)$ that affects the macromodel is amplified by μ^{-1}, possibly leading to highly inaccurate port signal estimates [27]–[32]. In this situation, we say that macromodel accuracy is *sensitive* to the actual termination condition. Conversely, a macromodel will be *robust* with respect to a particular termination network $\mathcal{L}$ when (6) hold *concurrently*.

The derivations in [31], [32] show that a straightforward solution to this problem is achieved by enforcing (4) together with the additional fitting condition

$$\mathbf{H}(s)\breve{\boldsymbol{x}}(s) \approx \breve{\boldsymbol{y}}(s), \tag{7}$$

where $\breve{\boldsymbol{x}}(s)$ and $\breve{\boldsymbol{y}}(s)$ are known from (3) as solutions of the nominal DUT under the prescribed termination condition. In practice, the starting point for the construction of a robust macromodel is a set of K frequency samples of the reference network function

$$\breve{\mathbf{H}}_k = \breve{\mathbf{H}}(j\omega_k), \quad k = 1, ..., K, \tag{8}$$

typically scattering responses computed by full-wave field solvers. In addition, we consider a set of M independent termination networks and associated sources

$$\mathcal{T}^{(m)} : \{\mathcal{L}^{(m)}, \boldsymbol{w}^{(m)}\}, \quad m = 1, \ldots, M. \tag{9}$$

For each of such termination networks we compute the nominal DUT port signals through a frequency-domain solution of (3), obtaining the signal pairs data

$$\breve{\boldsymbol{x}}_k^{(m)} = \breve{\boldsymbol{x}}^{(m)}(j\omega_k), \quad \breve{\boldsymbol{y}}_k^{(m)} = \breve{\boldsymbol{y}}^{(m)}(j\omega_k). \tag{10}$$

Then, a rational macromodel structure is assumed

$$\mathbf{H}(s) = \sum_{i=1}^{\nu} \frac{\mathbf{R}_i}{s - p_i} + \mathbf{R}_\infty, \tag{11}$$

where $\{p_i\}$ are the unknown model poles and $\{\mathbf{R}_i\}$ the corresponding unknown residue matrices with direct coupling $\mathbf{R}_\infty$. The robust model is identified through a standard VF pole relocation iteration, where the multiple fitting conditions

$$\mathbf{H}(j\omega_k) \approx \breve{\mathbf{H}}_k, \tag{12a}$$

$$\mathbf{H}(j\omega_k)\breve{\boldsymbol{x}}_k^{(m)} \approx \breve{\boldsymbol{y}}_k^{(m)}, \quad m = 1, \ldots, M, \tag{12b}$$

are enforced concurrently for $k = 1 \ldots K$ at each iteration. Technical details are given in [31, Sec. IV].

We remark that two application scenarios are enabled by this approach. If the application at hand requires fine-tuning the model accuracy for a well-defined termination condition, which is never modified during model operation, then one can set $M = 1$ and base model identification on that specific termination. There will be however no guarantee of reduced sensitivity under different operating conditions. If instead the model is requested to be robust to a possibly ample class of terminations, than multiple samples $M > 1$ from this class (9) will be needed, to reduce the likelihood of high sensitivity under varying termination conditions. The above statements are documented and illustrated through several examples in [31], [32]. A systematic procedure to design a *worst-case* termination that emphasizes sensitivity of a given DUT at one or more discrete frequencies is reported in the Appendix.

This manuscript completes this framework by proposing a PE post-processing that, combined with the above rational fitting scheme, produces a guaranteed passive model with enhanced robustness to terminations. In fact, application of any of the standard and well-documented passivity enforcement schemes to a robust macromodel will not preserve this robustness, thus spoiling all efforts previously spent to include termination effects in the rational fitting phase.

IV. Passivity enforcement

Starting from a stable macromodel in pole-residue form (11), a popular and effective method to enforce passivity consists in iteratively applying small perturbations to the model residues until suitable passivity constraints are met. This method will be referred to as *Standard PE* in the following and is described in full detail in [4, Sec. 10.5 and 10.10] and references therein.

In the following, we will assume that the macromodel representation $\mathbf{H}(s)$ is a scattering network function. Similar results hold for immittance representations, as for other passivity enforcement schemes. Under this assumption, a stable macromodel is passive if the transfer matrix norm is less than one [4], [34]–[36] for all frequencies

$$\|\mathbf{H}(j\omega)\| \leq 1, \qquad \forall\, \omega \in \mathbb{R}. \tag{13}$$

A non-passive macromodel would violate this constraint on N_v frequency bands $\Omega^{(i)}$, $i = 1, \ldots, N_v$, where its norm is above unity, that is

$$\|\mathbf{H}(j\omega)\| > 1, \quad \forall\, \omega \in \bigcup_{i=1}^{N_v} \Omega^{(i)}, \quad \Omega^{(i)} \triangleq (\omega_0^{(i)}, \omega_1^{(i)}) \tag{14}$$

where $\omega_0^{(i)}, \omega_1^{(i)}$ are the interval endpoints. A necessary condition for (13) is asymptotic passivity, i.e.

$$\|\mathbf{R}_\infty\| \leq 1. \tag{15}$$

In the following, we assume that condition (15) is enforced during the final residue estimation stage of the robust VF iteration introduced in [31]. This can be done easily via semidefinite optimization solvers, since (15) is convex in the unknown direct coupling term $\mathbf{R}_\infty$. Therefore, we assume that the violation intervals $\Omega^{(i)}$ are bounded.

The core idea behind residue perturbation-based PE algorithms [4] is to introduce a perturbation

$$\delta\mathbf{H}(s) = \sum_{i=1}^{\nu} \frac{\delta\mathbf{R}_i}{s - p_i} \tag{16}$$

such that the perturbed model $\mathbf{H}(s) + \delta\mathbf{H}(s) \triangleq \bar{\mathbf{H}}(s)$ is passive. Ideally, the model should be perturbed the least necessary to meet the constraints without impacting accuracy. These objectives can be encoded in an optimization problem where a cost function $J(\delta\mathbf{H})$ is minimized to find the optimal residue perturbation

$$\min_{\delta\mathbf{R}_i} J(\delta\mathbf{H}) \tag{17a}$$

$$\text{s.t. } \|\mathbf{H}(j\omega) + \delta\mathbf{H}(j\omega)\| \leq 1 \quad \forall\, \omega \in \mathbb{R} \tag{17b}$$

In principle, the constraint (17b) could be translated into a finite-dimensional Linear Matrix Inequality condition using the Kalman-Yakubovich-Popov (KYP) Lemma [37], and the

resulting problem would be solvable by semidefinite programming. However, computational complexity scales badly and makes this approach oftentimes impractical for many common applications where the modeled device has more than a few tens of ports and its model involves a modest number of poles. This intractability justifies an approximate approach to enforce the set of infinitely many constraints (17b) through its *discretized* version, namely a finite set of n_c passivity constraints localized at frequencies where (17b) is violated. In formulae, the constraint becomes

$$\left\|\bar{\mathbf{H}}(j\omega_\ell)\right\| \leq 1, \qquad \ell = 1, \ldots, n_c \tag{18}$$

where the set $\mathcal{C} = \{\omega_\ell\}_{\ell=1}^{n_c}$ is suitably chosen to target all frequency bands $\Omega^{(i)}$. For instance, these frequencies can be the mid-points of violation intervals. The consequence of enforcing the approximate constraint instead of (17b) is that new violations may appear in the perturbed model, at frequencies where passivity was not enforced. Hence, it is necessary to perform multiple PE steps iteratively, see [4], [19].

Given this overview, we shall now turn to a detailed description of the two crucial aspects of the residue perturbation-based PE algorithm, namely constraint formulation and the cost function. The only difference between the PE algorithm proposed here and standard passivity enforcement is indeed in the cost function $J(\delta\mathbf{H}(s))$, and this is discussed in the foregoing Sec. IV-A. Iterative formulation of localized constraints is the same as in standard PE and is reviewed in Sec. IV-B. Implementation details are provided in Sec. IV-C.

A. Cost function

The concurrent constraints (4) and (7) leading to a robust macromodel, suitably discretized as in (12), can be collected in a compact form and encoded in the following cost function

$$\begin{aligned} J_{\text{fit}} = &\sum_{k=1}^{K} \left\| \mathbf{H}(j\omega_k) - \breve{\mathbf{H}}_k \right\|_F^2 \\ &+ \lambda^2 \sum_{k=1}^{K} \left\| \mathbf{H}(j\omega_k)\breve{\mathbf{X}}_k - \breve{\mathbf{Y}}_k \right\|_F^2 \end{aligned} \tag{19}$$

where all input-output pairs $(\breve{\boldsymbol{x}}_k^{(m)}, \breve{\boldsymbol{y}}_k^{(m)})$ are collected in the following data matrices

$$\breve{\mathbf{X}}_k \triangleq \begin{pmatrix} \breve{\boldsymbol{x}}_k^{(1)} & \cdots & \breve{\boldsymbol{x}}_k^{(M)} \end{pmatrix} \tag{20a}$$

$$\breve{\mathbf{Y}}_k \triangleq \begin{pmatrix} \breve{\boldsymbol{y}}_k^{(1)} & \cdots & \breve{\boldsymbol{y}}_k^{(M)} \end{pmatrix} \tag{20b}$$

and where λ plays the role of a penalization parameter. In (19) the model error is optimized with respect to the original data samples of network function and port signals.

In a passivity enforcement based on structure (16), the model perturbation $\delta\mathbf{H}(s)$ depends linearly on the decision variables $\delta\mathbf{R}_i$. This suggests a formulation of the cost function for robust PE based on a local reference provided by the initial non-passive model rather than the raw data samples. This approach is standard in so-called *model-based* PE methods [4] and is here extended to account for the additional term in the enhanced cost function (19).

We need to ensure that the passive model $\bar{\mathbf{H}}(s)$ is robustly accurate based on both (4) and (7), which in this setting read

$$\bar{\mathbf{H}}(s) \approx \breve{\mathbf{H}}(s), \quad \bar{\mathbf{H}}(s)\breve{\boldsymbol{x}}(s) \approx \breve{\boldsymbol{y}}(s) \tag{21}$$

However, we know that the initial non-passive model obtained by minimizing (19) verifies (4) and (7). Combining with (21) this leads to

$$\bar{\mathbf{H}}(s) \approx \mathbf{H}(s), \quad \bar{\mathbf{H}}(s)\breve{\boldsymbol{x}}(s) \approx \mathbf{H}(s)\breve{\boldsymbol{x}}(s) \tag{22}$$

or equivalently

$$\delta\mathbf{H}(s) \approx 0, \quad \delta\mathbf{H}(s)\breve{\boldsymbol{x}}(s) \approx 0. \tag{23}$$

A discretization process (as described in Sec. III) leads to the proposed modified cost function for robust PE

$$J_{\text{PE}} = \sum_{k=1}^{K} \left(\|\delta\mathbf{H}(j\omega_k)\|_F^2 + \lambda^2 \left\| \delta\mathbf{H}(j\omega_k)\breve{\mathbf{X}}_k \right\|_F^2 \right). \tag{24}$$

where all frequency samples and all termination configurations (20a) are considered. Note that the above formulation does not require the data matrix (20b) and leads to a homogeneous cost function in the model perturbation. These two features are known to contribute to reducing computational cost on one side as well as improving convergence properties [4]. It should be noted that setting $\lambda = 0$ in (24), i.e., removing the second term in the proposed modified cost function J_{PE}, reduces the proposed formulation to the standard non-robust PE.

B. Passivity constraints

The constraint (17b) to be enforced for finding optimal perturbations is here approximated with a finite number of constraints (18), that are *localized* at a discrete set of frequencies $\{\omega_\ell\}_{\ell=1}^{n_c}$. Thus, an algorithmic method should be provided to identify this discrete set of frequencies at each PE iteration, based on the location of passivity violations, found through a *passivity check* stage. Several approaches are available for this task, either exploiting Hamiltonian spectral properties [21] or simpler adaptive sampling strategies [38]. This material is standard, see [4]. Therefore, we assume that the following passivity violation data are available

$$\{\sigma_{\ell,q}, \boldsymbol{u}_{\ell,q}, \boldsymbol{v}_{\ell,q}\}, \quad \ell = 1, \ldots, n_c, \quad q = 1, \ldots, Q_\ell \tag{25}$$

at frequencies ω_ℓ where the model $\mathbf{H}(j\omega_\ell)$ has Q_ℓ (one or more) singular values $\sigma_{\ell,q} > 1$, with associated left and right singular vectors $\boldsymbol{u}_{\ell,q}$, $\boldsymbol{v}_{\ell,q}$. In particular,

$$\boldsymbol{u}_{\ell,q}^* \mathbf{H}(j\omega_\ell)\boldsymbol{v}_{\ell,q} = \sigma_{\ell,q}\,, \quad \forall \ell, q. \tag{26}$$

Following [4], a first-order approximation of the perturbed singular value $\bar{\sigma}_{\ell,q}$ as a result of model perturbation can be written as

$$\bar{\sigma}_{\ell,q} \approx \sigma_{\ell,q} + \text{Re}\left\{ \boldsymbol{u}_{\ell,q}^* \delta\mathbf{H}(j\omega_\ell)\boldsymbol{v}_{\ell,q} \right\} \leq 1 \tag{27}$$

as $\|\delta\mathbf{H}\| \to 0$, which is required to be bounded by one. Assembling constraints (27) while minimizing the robust cost

function (24) leads to the proposed optimization problem for robust passivity enforcement

$$\min_{\delta\mathbf{R}_i} \sum_{k=1}^{K} \left(\|\delta\mathbf{H}(j\omega_k)\|_F^2 + \lambda^2 \left\| \delta\mathbf{H}(j\omega_k)\breve{\mathbf{X}}_k \right\|_F^2 \right) \tag{28a}$$

$$\text{s.t.} \quad \mathrm{Re}\left\{ \boldsymbol{u}_{\ell,q}^* \delta\mathbf{H}(j\omega_\ell)\boldsymbol{v}_{\ell,q} \right\} \leq 1 - \sigma_{\ell,q}, \quad \forall \ell, q \tag{28b}$$

C. Numerical implementation

In (28), the unknown model perturbation is represented by $\delta\mathbf{H}$, which is however induced by a perturbation on the model residues (16). Let us define a vector $\delta\boldsymbol{r}$ containing all the problem unknowns

$$\delta\boldsymbol{r} \triangleq \mathrm{vec}\left\{\delta\mathbf{R}\right\}, \text{ where } \delta\mathbf{R}^{\mathsf{T}} \triangleq \begin{pmatrix} \delta\mathbf{R}_1^{\mathsf{T}} & \cdots & \delta\mathbf{R}_\nu^{\mathsf{T}} \end{pmatrix} \tag{29}$$

We further define the Cauchy matrix $\boldsymbol{\Phi}$ with elements

$$[\boldsymbol{\Phi}]_{k,i} = (j\omega_k - p_i)^{-1}, \tag{30}$$

with its k-th row denoted as $\boldsymbol{\varphi}_k \in \mathbb{C}^{1\times\nu}$. The model perturbation (16) is first rewritten as

$$\delta\mathbf{H}(j\omega_\ell) = (\boldsymbol{\varphi}_\ell \otimes \mathbb{I}_P)\, \delta\mathbf{R}\,. \tag{31}$$

Using the properties of the Kronecker product allows restating each of the localized constraints (28b) in the following compact form

$$\begin{aligned} \boldsymbol{u}_{\ell,q}^* \delta\mathbf{H}(j\omega_\ell)\boldsymbol{v}_{\ell,q} &= (\boldsymbol{v}_{\ell,q}^{\mathsf{T}} \otimes \boldsymbol{u}_{\ell,q}^*)\, \mathrm{vec}\{\delta\mathbf{H}(j\omega_\ell)\} \\ &= (\boldsymbol{v}_{\ell,q}^{\mathsf{T}} \otimes \boldsymbol{u}_{\ell,q}^*)(\mathbb{I}_P \otimes \boldsymbol{\varphi}_\ell \otimes \mathbb{I}_P)\, \delta\boldsymbol{r} = \\ &= (\boldsymbol{v}_{\ell,q}^{\mathsf{T}} \otimes \boldsymbol{\varphi}_\ell \otimes \boldsymbol{u}_{\ell,q}^*)\, \delta\boldsymbol{r}\,. \end{aligned} \tag{32}$$

The model perturbations at all the sampled frequencies can be assembled from (31) as

$$\begin{pmatrix} \delta\mathbf{H}(j\omega_1) \\ \vdots \\ \delta\mathbf{H}(j\omega_K) \end{pmatrix} = (\boldsymbol{\Phi} \otimes \mathbb{I}_P)\, \delta\mathbf{R}\,. \tag{33}$$

This enables us to rewrite the cost function (24) in terms $\delta\boldsymbol{r}$. The first term in (24) can be compactly written as

$$\sum_{k=1}^{K} \|\delta\mathbf{H}(j\omega_k)\|_F^2 = \|(\mathbb{I}_P \otimes \boldsymbol{\Phi} \otimes \mathbb{I}_P)\, \delta\boldsymbol{r}\|^2\,. \tag{34}$$

As for the second term in (24), the contribution of the k-th frequency point can be written as

$$\mathrm{vec}\{\delta\mathbf{H}(j\omega_k)\breve{\mathbf{X}}_k\} = \underbrace{\left(\breve{\mathbf{X}}_k^{\mathsf{T}} \otimes \mathbb{I}_P\right)(\mathbb{I}_P \otimes \boldsymbol{\varphi}_k \otimes \mathbb{I}_P)}_{\triangleq \boldsymbol{\Psi}_k}\, \delta\boldsymbol{r}. \tag{35}$$

Upon substituting (34)-(35) in (24), J_{PE} becomes

$$\begin{aligned} J_{\mathrm{PE}} &= \|(\mathbb{I}_P \otimes \boldsymbol{\Phi} \otimes \mathbb{I}_P)\, \delta\boldsymbol{r}\|^2 + \lambda^2 \|\boldsymbol{\Psi}\delta\boldsymbol{r}\|^2 \\ &= \|\boldsymbol{\Theta}\, \delta\boldsymbol{r}\|^2 \end{aligned} \tag{36}$$

where $\boldsymbol{\Psi}$ stacks vertically the $\boldsymbol{\Psi}_k$ for $k = 1, \ldots, K$ as block-rows, and where

$$\boldsymbol{\Theta} = \begin{pmatrix} \mathbb{I}_P \otimes \boldsymbol{\Phi} \otimes \mathbb{I}_P \\ \lambda\boldsymbol{\Psi} \end{pmatrix} \tag{37}$$

plays the role of a *regressor* matrix, as in standard least squares problems. Thus, equations (36) and (32) respectively give the explicit dependence of (28a) and (28b) on the decision variables, leading to the optimization problem to be solved at each PE iteration

$$\min_{\delta\boldsymbol{r}} \|\boldsymbol{\Theta}\, \delta\boldsymbol{r}\|^2 \tag{38a}$$

$$\text{s.t.} \quad \mathrm{Re}\left\{ (\boldsymbol{v}_{\ell,q}^{\mathsf{T}} \otimes \boldsymbol{\varphi}_\ell \otimes \boldsymbol{u}_{\ell,q}^*)\delta\boldsymbol{r} \right\} \leq 1 - \sigma_{\ell,q}, \quad \forall\, \ell, q. \tag{38b}$$

The proposed robust PE scheme is summarized in Algorithm 1.

Algorithm 1 Robust Passivity Enforcement

Require: initial model $\mathbf{H}$, terminations $\mathcal{T}^{(m)}$ as in (9)
1: Run passivity check on $\mathbf{H}$ to find N_v violation bands $\Omega^{(i)}$
2: $\bar{\mathbf{H}} \leftarrow \mathbf{H}$
3: Compute regressor matrix $\boldsymbol{\Theta}$ of J_{PE} as in (37)
4: **while** $N_v > 0$ **do**
5: Select violation frequencies $\{\omega_\ell\}_{\ell=1}^{n_c}$ from all $\Omega^{(i)}$
6: **for** $\ell = 1, \ldots, n_c$ **do**
7: Compute $\{\sigma_{\ell,q} > 1, \boldsymbol{u}_{\ell,q}, \boldsymbol{v}_{\ell,q}\}$ as in (25)-(26)
8: Setup constraint matrices $\forall \ell, q$ as in (38b)
9: **end for**
10: Solve the minimization problem (38) to find $\delta\boldsymbol{r}$
11: $\bar{\mathbf{H}} \leftarrow \bar{\mathbf{H}} + \delta\mathbf{H}$, i.e. update residues based on (16)
12: Check passivity of $\bar{\mathbf{H}}$, retrieve N_v violation bands $\Omega^{(i)}$
13: **end while**
14: **return** $\bar{\mathbf{H}}$

D. Computational cost

The computational complexity of the proposed approach differs from that of standard PE schemes only for the increased row dimension of the matrix $\boldsymbol{\Theta} \in \mathbb{R}^{(M+P)PK\times P^2\nu}$, which depends on the possibly large number M of termination conditions included in the model optimization. This drawback can be alleviated by pre-processing $\boldsymbol{\Theta}$ before applying the robust PE scheme. This is possible because $\boldsymbol{\Theta}$ is block diagonal up to a permutation. Applying such permutation and computing the QR factorization of the resulting diagonal blocks allows to define the quadratic cost function of (38) in terms of a square block-diagonal matrix of size $P^2\nu$ (the total number of unknowns). This procedure is entirely analogue to the one described in [31] and originally in [10], to which the reader is referred for further details (additional implementation aspects are omitted here). The asymptotic computational cost of this pre-processing step is $O(MKP^3\nu^2)$. The impact of this overhead is quantified in Table I, which anticipates the runtime (including preliminary QR factorizations) and PE iterations that were experimentally measured for the three test cases presented in Sec. V on a workstation equipped with a Core i9-7900X CPU running at 3.3 GHz with 64 GB of RAM.

V. Numerical results

The advantages of the proposed robust PE scheme are illustrated on three different PDN testcases. Such structures are in fact known to be quite sensitive to port terminations when scattering-based rational macromodels are used in simulations at the system level.

This article has been accepted for publication in IEEE Transactions on Components, Packaging and Manufacturing Technology. This is the author's version which has not been fully edited content may change prior to final publication. Citation information: DOI 10.1109/TCPMT.2024.3407526

TABLE I
EXPERIMENTAL COMPARISON OF COMPUTATIONAL COST (STANDARD PE VS ROBUST PE) FOR THE THREE BENCHMARKS OF SEC. V.

			Runtime		# of iterations	
Example	P	ν	Standard	Robust	Standard	Robust
Sec. V-A	4	24	11.3 s	26 s	6	23
Sec. V-B	5	22	4.5 s	5.2 s	4	6
Sec. V-C	9	26	7.2 s	8.4 s	6	6

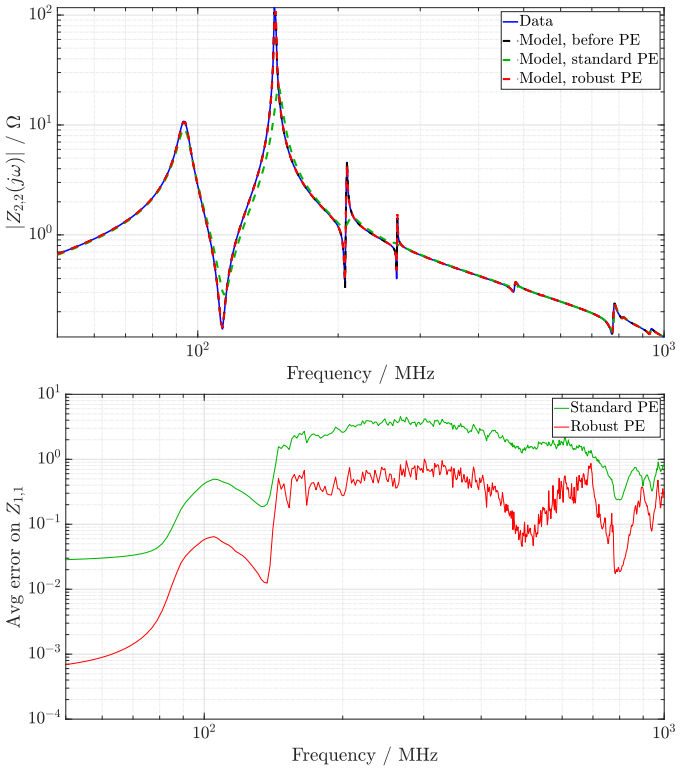

Fig. 2. Top panel: magnitude of the $Z_{2,2}$ entry of the impedance matrix of the canonical PDN example of Sec. V-A. The reference data is compared with the model response before PE, after standard PE, and after proposed robust PE. Bottom panel: Average absolute error on the $Z_{1,1}$ entry after loading DUT with 2000 random capacitive terminations.

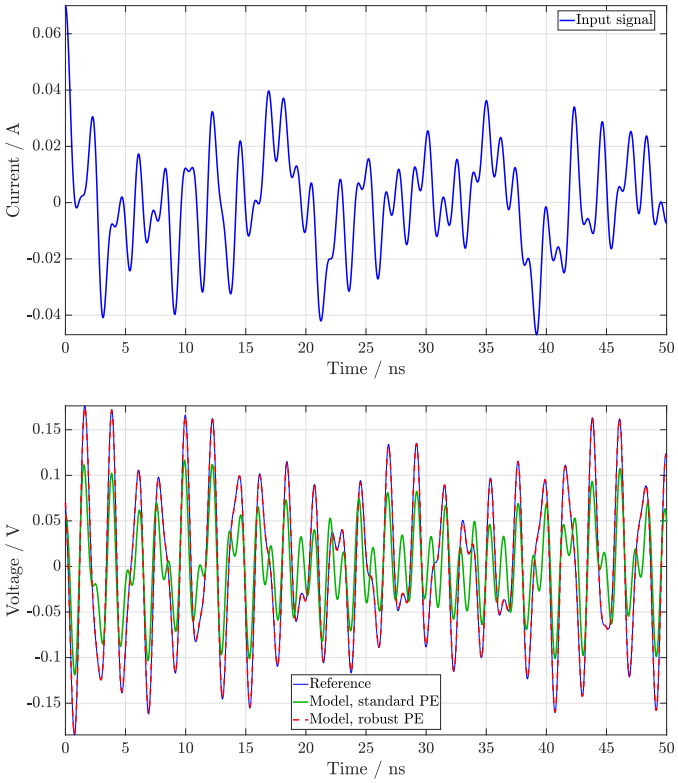

Fig. 3. Testcase A. Top panel: multi-sine current excitation signal; Bottom panel: port voltages obtained from macromodels after standard and robust PE.

A. Testcase A

This section describes a canonical PDN structure consisting in a pair of parallel conducting planes of size 12×10 cm separated by a 1 mm dielectric FR4 layer ($\epsilon_r = 4.7$, $\tan\delta = 0.01$). Five lumped ports are located at random plane locations, and one of them is connected to a 20 mΩ shunt resistor, so as to model the presence of a voltage regulator (VR) providing the main voltage and power supply. We consider the impedance matrix looking into the remaining four ports, for which a macromodel can be built. Note that this impedance matrix is well-defined at DC because of the low-impedance path provided by the resistive VR model.

This canonical example was already discussed in [31] as a template to demonstrate load sensitivity of standard VF models. This sensitivity arises when loading the four remaining ports with decoupling capacitors, which is a standard operation in PDN design. We apply the robust fitting algorithm reviewed in Sec. III to obtain a macromodel ($\nu = 24$ model poles and 20 VF iterations, $K = 2 \cdot 10^3$ data samples) that is robust with respect to such termination class, based on $M = 20$ random capacitive (RLC) loads. The R, L, C values of the capacitor models are uniformly distributed in the intervals $R \in [0.5, 1]\,\text{m}\Omega$, $L \in [5, 10]\,\text{pH}$, $C \in [5\,\text{pF}, 1\,\text{nF}]$. Next, model passivity is enforced by residue perturbation using both the standard cost function and the proposed robust cost function (38), with $n_c = 30$ passivity constraints in the first iteration. As a measure to verify improvements and reduced load sensitivity, we evaluate the 4×4 impedance matrix of the DUT, including a set of randomly-generated RLC shunt loads that were not used in the model training phase.

The top panel of Fig. 2 compares to the reference (exact) solution three different models. The robust model before PE (black line) is very accurate when compared to the exact solution. Standard PE degrades model accuracy after re-termination, as shown by the green dashed line. Using instead the proposed robust cost function in the PE phase provides superior accuracy (red dashed line). Such improvements are mostly visible in close proximity of the resonance peaks.

A statistical analysis is reported in the bottom panel of Fig. 2, which reports the average absolute error over frequency on the input impedance $Z_{1,1}$ when the macromodels are loaded with two thousand random capacitive terminations (drawn according to the same statistical distribution as the training ones). The proposed PE scheme gives a passive model that can be considered robust with a wide range of capacitive loads, so that the results displayed in the top panel of Fig. 2 hold consistently.

To further demonstrate the importance of a good approxima-

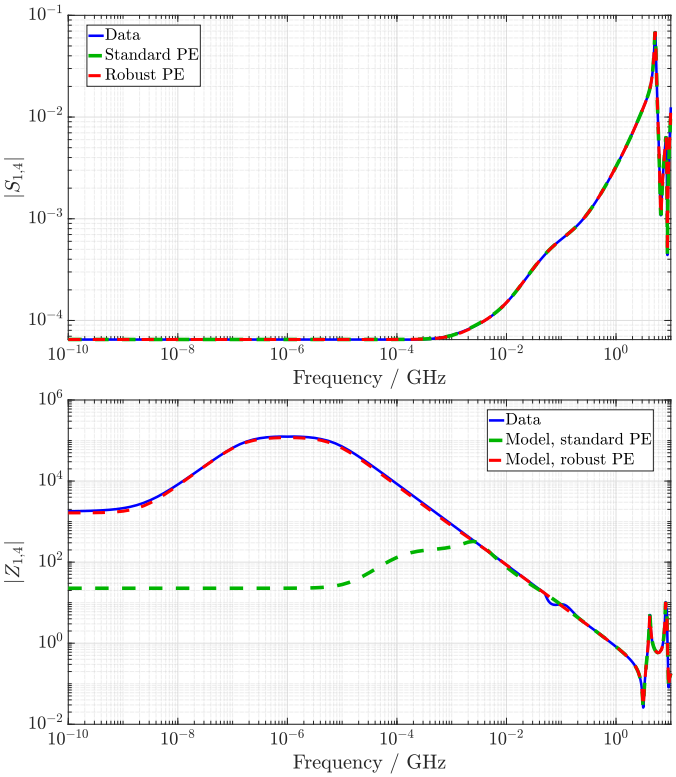

Fig. 4. Testcase B. Comparison of standard and robust passive macromodel responses to reference data. Top panel: selected scattering matrix response $S_{1,4}$. Bottom panel: selected impedance matrix response $Z_{1,4}$.

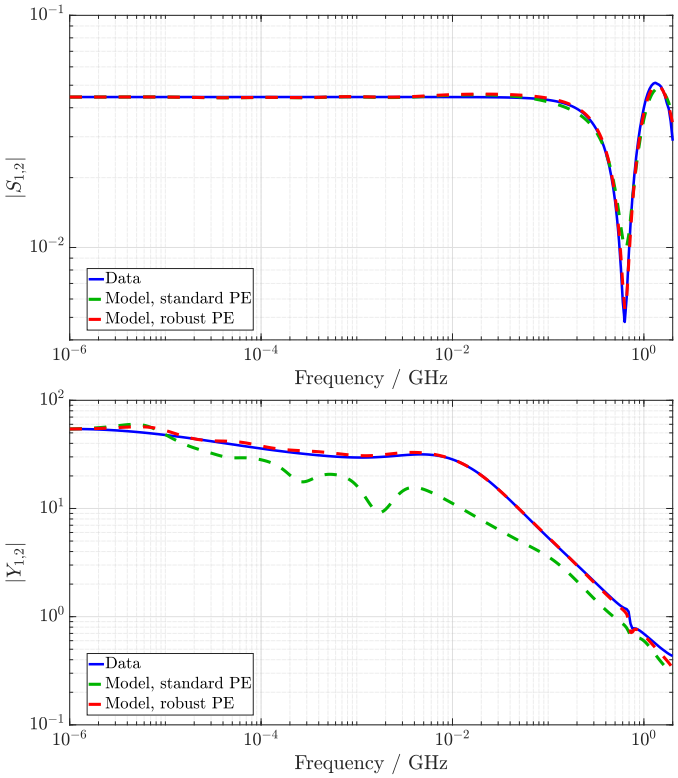

Fig. 5. Testcase C (5-port model). Comparison of macromodel responses after standard and robust PE to reference scattering responses (top panel) and after conversion to admittance representation (bottom panel).

tion of the reterminated input impedance, we look at the time-domain voltage response to a current stimulus. The top panel of Fig. 3 depicts the adopted current excitation, consisting in a superposition of seven sinewaves with different frequencies (corresponding to available ω_k) and equal amplitude (10 mA). This signal enables a trivial evaluation of an exact solution to be used as reference. The responses of the two passive models built using standard and robust cost function were computed as well. The bottom panel of Fig. 3 shows the excellent accuracy of the robust passive macromodel, whereas the standard macromodel exhibits unacceptable transient voltage errors. This results clearly demonstrate the practical importance and impact of using the newly defined J_{PE} to obtain robustly reliable results.

B. Testcase B

The second test case is an extraction of a real PDN with $P = 5$ modeled ports (courtesy of Jian Liu, Cadence). This structure shows strong error magnification when its macromodel, built in the native scattering representation ($R_0 = 1\,\Omega$), is converted to impedance (Z-parameters). The robust VF algorithm was first applied with $\nu = 22$ poles and 15 VF iterations to simultaneously optimize the S-parameters with $R_0 = 1\,\Omega$ and the Z-parameters (i.e. $M = 1$ termination scheme). The dataset contains $K = 1260$ samples. Given that the weighting coefficients (20) required to enforce the Z-parameters approximation are of much larger magnitude than the native scattering representation, we set the regularization parameter to $\lambda = 10^{-3}$. Then, we applied residue perturbation-based PE using the standard and the proposed robust cost functions, using $n_c = 9$ passivity constraints in the first iteration.

Results are depicted in Fig. 4. The top panel compares the two macromodels to the reference in terms of scattering parameters. All macromodels are accurate in this representation. However, when looking at the impedance responses in the bottom panel, we see that only the proposed PE formulation provides a model that remains robust against error amplification induced by the S-to-Z conversion. The impedance response of the standard model is severely incorrect. This implies that the standard model is practically useless in any system-level simulation setting, especially those adopting high-impedance terminations.

C. Testcase C

The last test case is extracted from an actual 45-port PDN package design [39]. We initially consider a subset of $P = 5$ ports to build an S-parameter macromodel that remains accurate when converted to the Y (admittance) representation. This requirement is not trivial, because for this particular example a standard VF macromodel exhibits high sensitivity in the S-to-Y conversion, as we will see below. Thus, we simultaneously fit the native scattering representation with $R_0 = 1\,\Omega$ while including weights (20) induced by the admittance parameter conversion ($M = 1$), using 14 poles and 15 VF iterations to fit $K = 317$ frequency samples. The resulting stable but

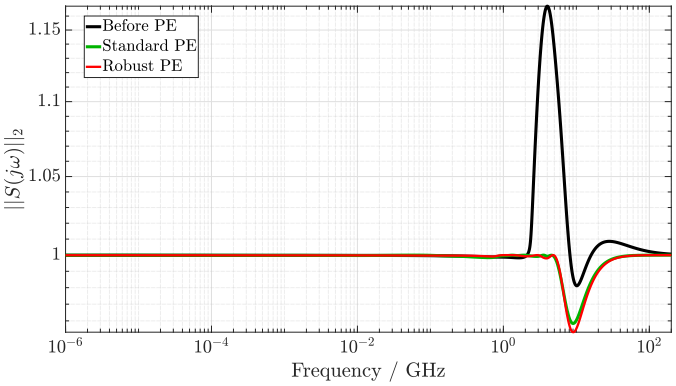

Fig. 6. Transfer matrix norm of the testcase considered in Sec. V-C, before and after PE. See Fig. 5 for the corresponding model responses.

non-passive model is the starting point for PE using standard and proposed robust implementations. At the first iteration, $n_c = 11$ constraints are enforced. The resulting S-parameter responses, reported in the top panel of Fig. 5, demonstrate that standard passivity enforcement works well in the native representation to which it is applied. However, conversion of the standard passive model to Y representation (Fig. 5, bottom panel) reveals major accuracy degradation. Conversely, the proposed robust PE scheme meets the expectations of preserving accuracy also in its admittance responses. Figure 6 reports the frequency-dependent norm $||\mathbf{S}(j\omega)||$ before and after PE, demonstrating that uniform passivity is achieved at all frequencies both for standard and robust implementations.

This package model is part of a larger PDN where it is connected to a prescribed set of terminations, including decoupling capacitors and a lumped VR model. Hence, it makes sense to build a model with optimized accuracy with respect to such prescribed loading network $\mathcal{L}$. To demonstrate the effectiveness of the proposed algorithm in achieving this purpose, we now focus on nine ports, where the loading-induced error magnification effect is particularly visible. A 9-port ($P = 9$) S-parameter macromodel was built using the robust VF algorithm with 26 poles and 20 VF iterations, whose representative scattering responses are displayed in Fig. 7 (top panel). Passivity was again enforced by residue perturbation using the standard PE, whose cost function does not take terminations into account, and the proposed robust PE (with $M = 1$). The resulting passive models are then loaded with decoupling capacitors and the input impedance of the re-terminated device is reported in Fig. 7 (bottom panel). This experiment confirms that the standard PE reintroduces the sensitivity issue (green dashed line), because its cost function minimizes the perturbation in S-parameters only (thus overlooking the error magnification issue), while the weighted PE seeks to perturb the model coefficients so as to retain accuracy of both the S-parameters and the input impedance after loading (red dashed line).

VI. Discussion

In this paper, we have documented how a simple modification of the cost function defining model accuracy leads to

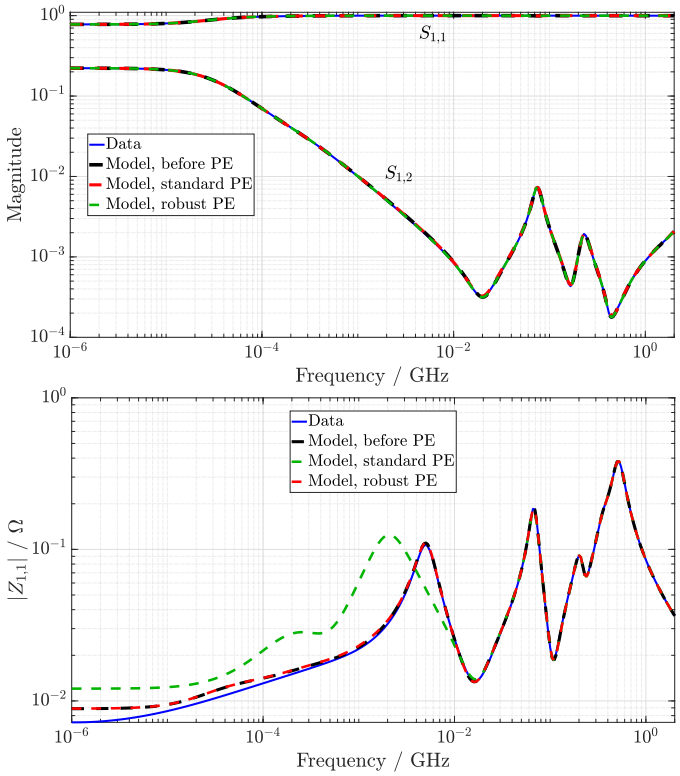

Fig. 7. Testcase C (9-port model). Comparison of passive model responses (standard and robust) to reference data. Top panel: direct comparison of scattering responses. Bottom panel: one representative PDN impedance matrix element after retermination with VR and decoupling capacitor models.

dramatic improvements in macromodel robustness to changes in its termination conditions. The presentation has been concentrated on a modification of a well-defined PE method [4, Sec. 10.5 and 10.10] which is reviewed in Sec. IV. More precisely, this approach is based on the iterative enforcement of discretized constraints enforcing bounded realness of the scattering macromodel response at a finite set of frequency points. In the Authors' opinion, this is by far the most effective PE approach among those based on perturbation, as demonstrated by the success of commercial tools (e.g. [40]) based on this method. Due to its good performance, this method has been successfully extended to the multivariate (parameterized) case, see e.g. [41], [42], where the various methods differ mainly on the strategy used to select the frequency locations $\{\omega_\ell\}$ where the local constraints are applied. Upon removing the external parameters and focusing on univariate (frequency-dependent) macromodels only, the latter methods are basically identical to the reference PE approach that is enhanced in this work. Therefore, it is expected that the adoption of the robust cost function proposed in this work in the multivariate setting of [41], [42] will lead to similar improvements on the sensitivity of parameterized macromodels. This investigation is left for future works.

A second remark is in order. Several strategies exist for PE, in addition to the local perturbation described in this work. Most notable approaches are the well-known methods based on Hamiltonian spectral perturbation [21] and those based on the KYP Lemma [22]. Such methods, thoroughly discussed

and compared in [4], are all based on the minimization of some cost function under specialized passivity constraints, respectively displacement of Hamiltonian eigenvalues or Linear Matrix Inequalities (LMIs) of KYP type. Such constraints can be directly combined with the proposed cost function, to make the corresponding PE methods robust to load variations. The local perturbation approach has been preferred in this work over KYP, because the latter would require the solution of a Semi-Definite optimization Program (SDP) with LMI constraints. Although SDP solvers are widely available and are being continuously improved, we found in our experiments the approach documented in this paper is numerically much more robust and can easily handle large-scale problems, whereas an SDP solver would be excessively demanding in terms of runtime and memory. An SDP-based PE equipped with the proposed robust cost function (24) was in fact implemented and used to enforce passivity of the 9-port model of Fig. 7 and Sec. V-C. This process required 1480 seconds, whereas the preferred local perturbation approach required only 8.4 s, with no appreciable difference in the results.

We conclude this section with a final remark on convergence. In this work, we have not considered Hamiltonian spectral perturbation approaches, since their specific constraints do not guarantee that the elimination of some passivity violation band will not generate another violation elsewhere. The only PE enforcement methods based on perturbation that guarantee convergence are those based on direct KYP constraints, which can be proved to be convex optimization problems in terms of the decision variables (residue perturbations). Unfortunately, as documented above, such methods are extremely demanding in terms of computing resources and are inapplicable on standard hardware to realistic large scale SI/PI structures. The PE framework that is adopted in this work is based on frequency-dependent constraints (13) that are fully equivalent to KYP constraints (under proper technical conditions, see [4]), which are discretized as (18) and linearized as (27). If the discretization is sufficiently dense and accurate, it is known that the resulting method preserves the good convergence properties of the KYP approach, with a dramatically reduced computational cost.

VII. Conclusions

This paper presented a systematic and effective approach to generate passive macromodels with reduced sensitivity to variations in their termination networks. The problem of load sensitivity is often overlooked in the rich literature on the subject. However, in the Authors' opinion such issue still represents a fundamental roadblock that prevents effective use of rational fitting algorithms in several application fields.

This paper completed the framework initially introduced in [31], where a robust formulation of the Vector Fitting scheme with reduced load sensitivity was presented. Here, a robust passivity enforcement scheme was presented, which, combined with the above robust VF, can lead to behavioral macromodels of LTI systems that are at the same time passive, hence unconditionally stable upon loading the macromodel with arbitrary passive termination networks, as well as robust to variations of such termination networks. Effectiveness of proposed algorithm was demonstrated on three Power Delivery Network benchmarks.

Appendix

In this section, we elaborate on the sensitivity of a given LTI system to its port terminations, and we propose a simple procedure to design a passive network that emphasizes such sensitivity. We denote such network as *worst-case termination*, not to be intended in strict sense, but rather as a particular load that maximizes sensitivity at one or more discrete frequencies by design.

Let us consider the setting of Fig. 1 and Sec. II, namely a DUT with input-output (scattering) representation (1) terminated into a passive LTI system (2). The solution for the interface port signals is reported in (3). Any modeling error $\Delta\mathbf{H}(s)$ in the approximation of $\breve{\mathbf{H}}(s)$ with a macromodel $\mathbf{H}(s)$ is amplified in the port signals by matrix $\mathbf{\Xi}^{-1}(s)$ where

$$\mathbf{\Xi}(s) = \mathbb{I}_P - \mathbf{\Gamma}(s)\breve{\mathbf{H}}(s). \tag{39}$$

We attempt designing a passive P-port network with scattering matrix $\mathbf{\Gamma}(s)$ that maximizes the magnitude of the largest eigenvalue of $\mathbf{\Xi}^{-1}(s)$, which is equivalent to minimizing the magnitude of the smallest eigenvalue of $\mathbf{\Xi}(s)$.

Let us consider a fixed frequency $s_0 = j\omega_0$ and perform a singular value decomposition of the DUT scattering matrix

$$\breve{\mathbf{H}}(s_0) = \mathbf{U}_0\mathbf{\Sigma}_0\mathbf{V}_0^* = \sum_{i=1}^{P} \sigma_{0,i}\boldsymbol{u}_{0,i}\boldsymbol{v}_{0,i}^* \tag{40}$$

with sorted singular values $\sigma_{0,i} \geq \sigma_{0,i+1}$ and mutually orthonormal left (right) singular vectors $\boldsymbol{u}_{0,i}$ ($\boldsymbol{v}_{0,i}$). Given the assumption that the DUT is passive, we have $\sigma_{0,1} \leq 1$, $\forall\omega_0$. We then define a rank-one matrix

$$\mathbf{\Gamma}(s_0) = \mathbf{\Gamma}_0 = \alpha_{0,1}\boldsymbol{v}_{0,1}\boldsymbol{u}_{0,1}^*. \tag{41}$$

Replacing (40) and (41) in (39) leads to

$$\begin{aligned}\mathbf{\Xi}(s_0) &= \mathbb{I}_P - \alpha_{0,1}\boldsymbol{v}_{0,1}\boldsymbol{u}_{0,1}^* \sum_{i=1}^{P} \sigma_{0,i}\boldsymbol{u}_{0,i}\boldsymbol{v}_{0,i}^* \\ &= \mathbb{I}_P - \alpha_{0,1}\sigma_{0,1}\boldsymbol{v}_{0,1}\boldsymbol{v}_{0,1}^*\end{aligned} \tag{42}$$

from which we see that one eigenvalue of $\mathbf{\Xi}(s_0)$ is equal to $\mu_{0,1} = 1 - \alpha_{0,1}\sigma_{0,1}$. The minimum value that can be attained by this eigenvalue under the constraint that also $\mathbf{\Gamma}(s)$ is a passive LTI network (with $\alpha_{0,1} \leq 1$) occurs when $\alpha_{0,1} = 1$ and reads $\mu_{0,1} = 1 - \sigma_{0,1}$. This value is minimum at the frequency ω_0 where $\sigma_{0,1}$ is largest. The above considerations lead to the following procedure:

1) find the frequency ω_0 that maximizes $\sigma_{0,1} = \|\breve{\mathbf{H}}(j\omega_0)\|$
2) assemble the rank-one matrix (41) with $\alpha_{0,1} = 1$, namely
$$\mathbf{\Gamma}_0 = \boldsymbol{v}_{0,1}\boldsymbol{u}_{0,1}^* \tag{43}$$
3) find a real stable rational matrix function $\mathbf{\Gamma}(s)$ that interpolates $\mathbf{\Gamma}_0$ at $s = j\omega_0$ while satisfying the passivity condition $\|\mathbf{\Gamma}(j\omega)\| \leq 1,\ \forall\omega \in \mathbb{R}$.

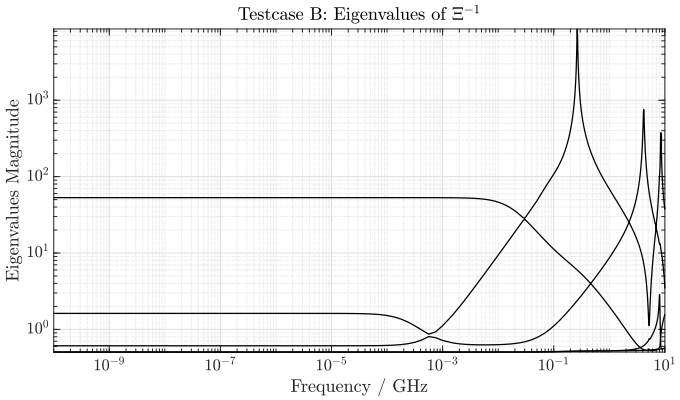

Fig. 8. Error amplification factor for testcase B under loading with its worst-case termination network.

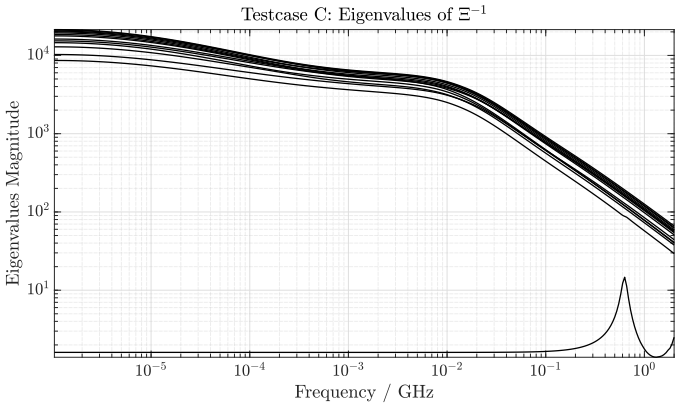

Fig. 9. As in Fig. 8, but for testcase C.

The resulting $\mathbf{\Gamma}(s)$ provides the worst-case termination at frequency ω_0. The following generalizations can be envisioned

- if the largest singular value $\sigma_{0,1}$ has multiplicity m higher than one, or similarly if m singular values are very close to 1, then a rank-m matrix $\mathbf{\Gamma}_0$ can be defined as
$$\mathbf{\Gamma}_0 = \sum_{i=1}^{m} \boldsymbol{v}_{0,i} \boldsymbol{u}_{0,i}^* \tag{44}$$
resulting in multiple eigenvalues $\mu_{0,i} = 1 - \sigma_{0,i}$;
- if there are multiple frequencies $j\omega_k$ at which $\sigma_{k,1} = \|\check{\mathbf{H}}(j\omega_k)\|$ are very close to one, than rank-1 or rank-m matrices $\mathbf{\Gamma}_k$ can be defined as in (43) or (44) and used to construct a passive rational matrix $\mathbf{\Gamma}(s)$ that interpolates all such $\mathbf{\Gamma}_k$. The resulting termination network will emphasize sensitivity at all frequencies ω_k.

Circuit synthesis of $\mathbf{\Gamma}(s)$ can be performed using the general methods discussed in [4] or [24].

We illustrate the above process with two examples, namely the testcases B and C discussed in Sec. V-B and Sec. V-C, respectively. Figures 8 and 9 report the frequency-dependent eigenvalues of $\mathbf{\Xi}^{-1}(j\omega)$ based on the worst-case terminations designed at DC and at some high-frequency point. In both cases the largest eigenvalue reaches a value of $\approx 10^4$, denoting high sensitivity and error magnification. The theory and algorithms presented in this work demonstrate that, by embedding such terminations in the fitting and passivity enforcement cost functions, the resulting macromodel will remain accurate also under such worst-case terminations.

REFERENCES

[1] R. Achar and M. S. Nakhla, "Simulation of high-speed interconnects," *Proceedings of the IEEE*, vol. 89, no. 5, pp. 693–728, May 2001.

[2] A. Carlucci, T. Bradde, S. Grivet-Talocia, S. Mongrain, S. Kulasekaran, and K. Radhakrishnan, "A compressed multivariate macromodeling framework for fast transient verification of system-level power delivery networks," *IEEE Transactions on Components, Packaging and Manufacturing Technology*, vol. 13, no. 10, pp. 1553–1566, 2023.

[3] A. Carlucci, S. Grivet-Talocia, S. Kulasekaran, and K. Radhakrishnan, "Structured model order reduction of system-level power delivery networks," *IEEE Access*, vol. 12, pp. 18 198–18 214, 2024.

[4] S. Grivet-Talocia and B. Gustavsen, *Passive Macromodeling: Theory and Applications*. New York: John Wiley and Sons, 2016 (published online on Dec 7, 2015).

[5] B. Gustavsen and A. Semlyen, "Rational approximation of frequency domain responses by vector fitting," *Power Delivery, IEEE Transactions on*, vol. 14, no. 3, pp. 1052–1061, jul 1999.

[6] B. Gustavsen, "Relaxed vector fitting algorithm for rational approximation of frequency domain responses," in *Signal Propagation on Interconnects, 2006. IEEE Workshop on*, may 2006, pp. 97–100.

[7] S. Lefteriu and A. C. Antoulas, "On the convergence of the vector-fitting algorithm," *Microwave Theory and Techniques, IEEE Transactions on*, vol. 61, no. 4, pp. 1435–1443, 2013.

[8] D. Deschrijver, B. Haegeman, and T. Dhaene, "Orthonormal vector fitting: A robust macromodeling tool for rational approximation of frequency domain responses," *Advanced Packaging, IEEE Transactions on*, vol. 30, no. 2, pp. 216–225, may 2007.

[9] S. Grivet-Talocia and M. Bandinu, "Improving the convergence of vector fitting for equivalent circuit extraction from noisy frequency responses," *IEEE Trans. Electromagnetic Compatibility*, vol. 48, no. 1, pp. 104–120, February 2006.

[10] D. Deschrijver, M. Mrozowski, T. Dhaene, and D. De Zutter, "Macromodeling of multiport systems using a fast implementation of the vector fitting method," *Microwave and Wireless Components Letters, IEEE*, vol. 18, no. 6, pp. 383–385, june 2008.

[11] A. Chinea and S. Grivet-Talocia, "On the parallelization of vector fitting algorithms," *IEEE Transactions on Components, Packaging and Manufacturing Technology*, vol. 1, no. 11, pp. 1761–1773, November 2011.

[12] S. Ganeshan, N. K. Elumalai, R. Achar, and W. K. Lee, "Gvf: Gpu-based vector fitting for modeling of multiport tabulated data networks," *IEEE Transactions on Components, Packaging and Manufacturing Technology*, vol. 10, no. 8, pp. 1375–1387, 2020.

[13] C.-C. Chou and J. E. Schutt-Ainé, "On the acceleration of the vector fitting for multiport large-scale macromodeling," *IEEE Microwave and Wireless Components Letters*, vol. 31, no. 1, pp. 1–4, 2021.

[14] B. Gustavsen and C. Heitz, "Rational modeling of multiport systems by modal vector fitting," in *Signal Propagation on Interconnects, 2007. SPI 2007. IEEE Workshop on*, may 2007, pp. 49–52.

[15] S. Grivet-Talocia, "Package macromodeling via time-domain vector fitting," *IEEE Microwave and Wireless Components Letters*, vol. 13, no. 11, pp. 472–474, November 2003.

[16] T. Bradde, S. Chevalier, M. De Stefano, S. Grivet-Talocia, and L. Daniel, "Handling initial conditions in vector fitting for real time modeling of power system dynamics," *Energies*, vol. 14, no. 9, 2021. [Online]. Available: https://www.mdpi.com/1996-1073/14/9/2471

[17] T. Bradde and S. Grivet-Talocia, "A comprehensive framework for training stable and passive multivariate behavioral models," in *2023 IEEE 27th Workshop on Signal and Power Integrity (SPI)*, 2023, pp. 1–4.

[18] B. Gustavsen and A. Semlyen, "Enforcing passivity for admittance matrices approximated by rational functions," *Power Engineering Review, IEEE*, vol. 21, no. 2, p. 54, feb. 2001.

[19] S. Grivet-Talocia and A. Ubolli, "A comparative study of passivity enforcement schemes for linear lumped macromodels," *IEEE Trans. Advanced Packaging*, vol. 31, no. 4, pp. 673–683, Nov 2008.

[20] B. Gustavsen, "Fast passivity enforcement of rational macromodels by perturbation of residue matrix eigenvalues," in *Signal Propagation on Interconnects, 2007. SPI 2007. IEEE Workshop on*, may 2007, pp. 71–74.

[21] S. Grivet-Talocia, "Passivity enforcement via perturbation of Hamitonian matrices," *IEEE Trans. Circuits and Systems I: Fundamental Theory and Applications*, vol. 51, no. 9, pp. 1755–1769, September 2004.

[22] C. P. Coelho, J. Phillips, and L. M. Silveira, "A convex programming approach for generating guaranteed passive approximations to tabulated frequency-data," *Computer-Aided Design of Integrated Circuits and Systems, IEEE Transactions on*, vol. 23, no. 2, pp. 293 – 301, feb. 2004.

[23] T. Dhaene, D. Deschrijver, and N. Stevens, "Efficient algorithm for passivity enforcement of S-parameter-based macromodels," *Microwave Theory and Techniques, IEEE Transactions on*, vol. 57, no. 2, pp. 415–420, Feb 2009.

[24] S. Grivet-Talocia, "On driving non-passive macromodels to instability," *International Journal of Circuit Theory and Applications*, vol. 37, no. 8, pp. 863–886, Oct 2009.

[25] M. Swaminathan, D. Chung, S. Grivet-Talocia, K. Bharath, V. Laddha, and J. Xie, "Designing and modeling for power integrity," *IEEE Transactions on Electromagnetic Compatibility*, vol. 52, no. 2, pp. 288–310, May 2010.

[26] K. Radhakrishnan, M. Swaminathan, and B. K. Bhattacharyya, "Power delivery for high-performance microprocessors—challenges, solutions, and future trends," *IEEE Transactions on Components, Packaging and Manufacturing Technology*, vol. 11, no. 4, pp. 655–671, 2021.

[27] B. Gustavsen, "Rational modeling of multiport systems via a symmetry and passivity preserving mode-revealing transformation," *Power Delivery, IEEE Transactions on*, vol. 29, no. 1, pp. 199–206, Feb 2014.

[28] B. Gustavsen and C. Heitz, "Modal vector fitting: A tool for generating rational models of high accuracy with arbitrary terminal conditions," *Advanced Packaging, IEEE Transactions on*, vol. 31, no. 4, pp. 664–672, nov. 2008.

[29] A. Ubolli, S. Grivet-Talocia, M. Bandinu, and A. Chinea, "Sensitivity-based weighting for passivity enforcement of linear macromodels in power integrity applications," in *2014 Design, Automation & Test in Europe Conference & Exhibition (DATE), Dresden, Germany, 24–28 Mar*, 2014, pp. 1–6.

[30] S. Grivet-Talocia, A. Ubolli, M. Bandinu, and A. Chinea, "An iterative reweighting process for macromodel extraction of power distribution networks," in *2013 IEEE 22nd Conference on Electrical Performance of Electronic Packaging and Systems*, 2013, pp. 125–128.

[31] A. Carlucci, T. Bradde, and S. Grivet-Talocia, "Addressing load sensitivity of rational macromodels," *IEEE Transactions on Components, Packaging and Manufacturing Technology*, vol. 13, no. 10, pp. 1591–1602, 2023.

[32] ——, "Improving accuracy of rational macromodels under realistic loading conditions," in *2023 IEEE 32nd Conference on Electrical Performance of Electronic Packaging and Systems (EPEPS)*, 2023, pp. 1–3.

[33] B. Gustavsen, "Passivity enforcement by residue perturbation via constrained non-negative least squares," *IEEE Transactions on Power Delivery*, vol. 36, no. 5, pp. 2758–2767, 2021.

[34] M. R. Wohlers, *Lumped and Distributed Passive Networks*. Academic press, 1969.

[35] S. Boyd, L. El Ghaoui, E. Feron, and V. Balakrishnan, *Linear matrix inequalities in system and control theory*. Society for Industrial and Applied Mathematics, 1994, vol. 15.

[36] S. P. Boyd and L. Vandenberghe, *Convex optimization*. Cambridge University Press, 2004.

[37] A. Rantzer, "On the kalman—yakubovich—popov lemma," *Systems & Control Letters*, vol. 28, no. 1, pp. 7–10, 1996. [Online]. Available: https://www.sciencedirect.com/science/article/pii/0167691195000631

[38] M. De Stefano, S. Grivet-Talocia, T. Wendt, C. Yang, and C. Schuster, "A multistage adaptive sampling scheme for passivity characterization of large-scale macromodels," *IEEE Transactions on Components, Packaging and Manufacturing Technology*, vol. 11, no. 3, pp. 471–484, 2021.

[39] A. Chinea, S. Grivet-Talocia, D. Deschrijver, T. Dhaene, and L. Knockaert, "On the construction of guaranteed passive macromodels for high-speed channels," in *DATE 2010 - Design, Automation and Test in Europe, Dresden, Germany*, March 8–12, 2010, pp. 1142–1147.

[40] "IdEM R2018, Dassault Systèmes." [Online]. Available: www.3ds.com/products-services/simulia/products/idem/

[41] A. Zanco, S. Grivet-Talocia, T. Bradde, and M. De Stefano, "Enforcing passivity of parameterized LTI macromodels via hamiltonian-driven multivariate adaptive sampling," *IEEE Transactions on Computer-Aided Design of Integrated Circuits and Systems*, vol. 39, no. 1, pp. 225–238, Jan 2020.

[42] S. Grivet-Talocia, "A perturbation scheme for passivity verification and enforcement of parameterized macromodels," *IEEE Transactions on Components, Packaging and Manufacturing Technology*, vol. 7, no. 11, pp. 1869–1881, Nov 2017.

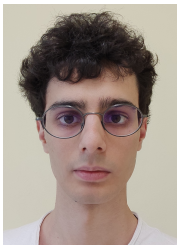

Antonio Carlucci (Graduate Student Member, IEEE) received the B.Sc. and M.Sc. degrees in Electronic Engineering respectively in 2019 and 2021, both from Politecnico di Torino, Turin, Italy, where he is currently pursuing a Ph.D. degree within the EMC group. His research focuses on large-scale simulation of electronic systems using macromodeling methods. He received the Best Student Paper award of SPI 2023, the 27th IEEE Workshop on Signal and Power Integrity.

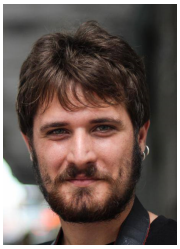

Tommaso Bradde (Member,IEEE) received the B.Sc. degree in Electronic Engineering from Roma Tre University, Rome, Italy, in 2015, the M.Sc. degree in Mechatronic Engineering from Politecnico di Torino, Turin, Italy, in 2018, and the Ph.D. degree in Electrical, Electronic and Communications Engineering from Politecnico di Torino, Turin, Italy, in 2022. He is currently a researcher and Assistant Professor with the Politecnico di Torino. His current research is focused on data-driven parameterized macromodeling and its applications to system level signal and power integrity assesments, with the inclusion of active devices. He is co-recipient of the 2018 Best Paper Award of the IEEE International Symposium on Electromagnetic Compatibility, of the 2020 and 2022 Best Paper Awards of the IEEE Conference on Electrical Performance of Electronic Packaging and Systems, and of the Best Student Paper Award of the 23rd IEEE workshop on Signal and Power Integrity.

Stefano Grivet-Talocia (M'98–SM'07–F'18) received the Laurea and Ph.D. degrees in electronic engineering from the Politecnico di Torino, Turin, Italy in 1994 and 1998, respectively. From 1994 to 1996, he was with the NASA/Goddard Space Flight Center, Greenbelt, MD, USA. He is currently a Full Professor of electrical engineering with the Politecnico di Torino. He co-founded the academic spinoff company IdemWorks (Turin, Italy) in 2007, serving as the President until its acquisition by CST in 2016. He has authored about 200 journal and conference papers. His current research interests include passive macromodeling of lumped and distributed interconnect structures, model-order reduction, modeling and simulation of fields, circuits, and their interaction, wavelets, time-frequency transforms, and their applications. Dr. Grivet-Talocia was a co-recipient of the 2007 Best Paper Award of the IEEE TRANSACTIONS ON ADVANCED PACKAGING. He received the IBM Shared University Research Award in 2007, 2008, and 2009 and an Intel Strategic Research Segment Grant in 2022, 2023 and 2024. He was an Associate Editor of the IEEE TRANSACTIONS ON ELECTROMAGNETIC COMPATIBILITY from 1999 to 2001 and He is currently serving as Associate Editor for the IEEE TRANSACTIONS ON COMPONENTS, PACKAGING AND MANUFACTURING TECHNOLOGY. He was the General Chair of the 20th and 21st IEEE Workshops on Signal and Power Integrity (SPI2016 and SPI2017), the co-Chair of SPI2023 and the Program co-Chair of SPI2024.